Translational Hydration Water Dynamics Drives the Protein Glass Transition

Alexander L. Tournier, Jiancong Xu, and Jeremy C. Smith
Interdisciplinary Center for Scientific Computing (IWR), Universität Heidelberg, 69120 Heidelberg, Germany

ABSTRACT Experimental and computer simulation studies have revealed the presence of a glasslike transition in the internal dynamics of hydrated proteins at ~200 K involving an increase of the amplitude of anharmonic dynamics. This increase in flexibility has been correlated with the onset of protein activity. Here, we determine the driving force behind the protein transition by performing molecular dynamics simulations of myoglobin surrounded by a shell of water. A dual heatbath method is used with which, in any given simulation, the protein and solvent are held at different temperatures, and sets of simulations are performed varying the temperature of the components. The results show that the protein transition is driven by a dynamical transition in the hydration water that induces increased fluctuations primarily in side chains in the external regions of the protein. The water transition involves activation of translational diffusion and occurs even in simulations where the protein atoms are held fixed.

INTRODUCTION

A variety of experiments have demonstrated the existence of a dynamical transition in hydrated proteins at ~180–220 K, characterized by deviation from linearity of the temperature dependence of the mean-square displacement, $\langle u^2 \rangle$ (Cohen et al., 1981; Parak et al., 1981; Knapp et al., 1982; Doster et al., 1989, 1990; Rasmussen et al., 1992; Tilton et al., 1992; Ferrand et al., 1993; Green et al., 1994; Fitter et al., 1997; Reat et al., 2000; Bicout and Zaccai, 2001; Lee and Wand, 2001; Teeter et al., 2001). The protein transition has dynamical aspects in common with the liquid-glass transition. For example, as in glass-forming liquids, proteins exhibit diffusive motions above the transition and are trapped in harmonic potential wells below. Experiments have shown that in several proteins biological function ceases below the dynamical transition (Parak et al., 1980; Rasmussen et al., 1992; Ferrand et al., 1993).

An important physical question concerns the environmental effect on the dynamical transition. Molecular dynamics (MD) simulations (Smith et al., 1990; Hayward and Smith, 2002) and neutron scattering experiments (Paciaroni et al., 2002) have shown that isolated or dehydrated proteins present dynamical transition behavior. However, a number of experiments and simulations have indicated that when a protein is solvated the dynamical transition is strongly coupled to the solvent (Ferrand et al., 1993; Steinbach and Brooks, 1993, 1996; Fitter et al., 1997; Cordone et al., 1999; Fitter, 1999; Reat et al., 2000; Tarek and Tobias, 2000, 2002; Teeter et al., 2001; Caliskan et al., 2002; Paciaroni et al., 2002). Highly viscous solvents, such as trehalose, suppress dynamical transition behavior (Hagen et al., 1995; Cordone et al., 1999; Walser et al., 2000), and neutron scattering experiments on enzymes in a range of cryosolvents showed that the dynamical transition behavior of the protein solution resembles that of the pure solvent (Bizzarri et al., 2000; Reat et al., 2000).

The observed solvent coupling leads to the question of whether the dynamical transition in a solvated protein is controlled by the solvent or whether the intrinsic anharmonicity of protein dynamics also plays a role. To investigate this, dual heatbath MD simulations can be used, in which the solvent and protein are held at different temperatures. Dual heatbath simulations have previously demonstrated that cold solvent strongly inhibits internal protein fluctuations, whereas hot solvent increases them (Vitkup et al., 2000). Here, we report on the results of several sets of dual heatbath simulations of a hydrated protein, myoglobin. Varying the temperature of one component (protein or solvent) while keeping the other temperature constant dissociates changes with temperature of features of the protein energy landscape from those inherent to the solvent. This enables the driving force behind the protein transition to be identified.

METHODS

Model system and potential function

The CHARMM program (Brooks et al., 1983) version 27b2 was used to perform the simulations. The model system constructed and the potential function were that of Vitkup et al. (2000). The model consists of one myoglobin molecule surrounded by a shell of water molecules, constructed by placing the protein in a box of water and retaining those 492 water molecules closest to the protein. The model system mimics the hydrated powder sample used in neutron scattering experiments in Doster et al. (1989), for which it was shown that dynamical transition behavior occurs on a timescale well sampled by the present calculations, i.e., $<10^{-10}$ s. The myoglobin coordinates were taken from the Protein Data Bank (from www.rscb.org) structure 1A6G, solved at 1.15 Å resolution using x-ray crystallography (Vojtechovsky et al., 1999). The TIP3P potential function was used to model the water molecules (Jorgensen et al., 1983), and the CHARMM all-atom parameter set 22 was used for the protein (MacKerell et al., 1998). As in Vitkup et al. (2000), a shift function with a 12 Å cutoff was used to truncate the electrostatic interactions, and a switch function was used to truncate the van der Waals contributions over 10–12 Å. A relative

Submitted December 5, 2002, and accepted for publication May 20, 2003.

Address reprint requests to Jeremy C. Smith, Interdisciplinary Center for Scientific Computing (IWR), Im Neuenheimer Feld 368, Universität Heidelberg, 69120 Heidelberg, Germany.

0006-3495/03/09/1871/05 $2.00

dielectric constant of 1 was used. A time step of 1 fs was employed for the MD simulations.

All simulations were performed with the same protocol. To relax the water shell, the system was subjected to energy minimization with harmonic constraints on the protein atoms followed by 5 ps MD heating up to 180 K with the protein atoms fixed and 5 ps equilibration with harmonic constraints on the protein atoms. Subsequently all constraints were removed, and 5 ps equilibration of the whole system at 180 K was performed followed by Adopted Basis Newton-Raphson energy minimization (Brooks et al., 1983). The system was then again heated to 180 K over 5 ps. In a further phase of heating, the protein and solvent were brought to their desired temperatures in 5 K increments every 200 fs, and the system was equilibrated for 20 ps. The subsequent production phase was 200 ps long for each simulation, and the data from this phase were used for the analysis. No instabilities were present in the simulations, and the maximal root-mean-square deviation of backbone heavy atoms with respect to the crystallographic structure was 1.15 Å, indicating that the protein structure remained stable.

Dual heatbath molecular dynamics

In dual heatbath methods, both subsystems are connected to a different heatbath characterized by a different reference temperature. Here, the Nosé-Hoover Chain (NHC) method was used for the dual heatbath calculations, in which the different parts of the system are each regulated not by one but by two heatbaths, the first one regulating the system and the second regulating the first heatbath (Martyna et al., 1996). NHC has the advantages over the original Nosé-Hoover algorithm (Hoover, 1985) that exact canonical behavior is reproduced, and the simulations are not prone to unphysical temperature oscillations (Holian et al., 1995). The NHC algorithm was employed using multiple time steps and Yoshida-Suzuki integration steps as described in Martyna et al., 1996. The characteristic time for the thermostat motion adopted was 0.2 ps, a value commonly used for condensed phase molecular systems. With the above method, the variation of the protein surface temperature was found not to exceed 10 degrees in all simulations except those in which the solvent was held at 300 K. For the solvent 300 K simulations, at low temperatures there was a temperature gradient leading to significant heating of the protein surface, the most extreme case being a surface heating of 40 degrees in the protein 80 K/solvent 300 K simulation. Although this surface heating was found not to significantly alter the average fluctuation properties examined here, an additional set of solvent 300 K simulations was performed with improved surface temperature properties. To do this, three shells were used: the solvent, the protein surface (protein atoms less than 2.5 Å from any water atom), and the rest of the protein. This led to a temperature stability of the surface residues of 2 degrees. The results from this set of simulations are those shown in Fig. 1 *b*.

Eight sets of simulations were performed. In six of these, the protein or the solvent temperature was held at 80, 180, or 300 K while varying the temperature of the other component from 80 K to 300 K in 20 K steps below 140 K and 10 K steps above 140 K. In a seventh set of simulations, the protein atoms were fixed and the solvent temperature varied from 80 to 300 K. Finally, a ''control'' set of simulations was also performed with the solvent and protein held at the same temperature. Each simulation required 8 h on 4 processors (800 MHz) in a Linux cluster. The 100 simulations performed required ~3200 h of CPU.

RESULTS

Fig. 1 *a* presents the protein fluctuations calculated from the control set of simulations (in each simulation the protein and solvent are at the same temperature), together with those obtained by fixing the temperature of one component at a temperature below the dynamical transition while varying the temperature of the other. In the control set, the

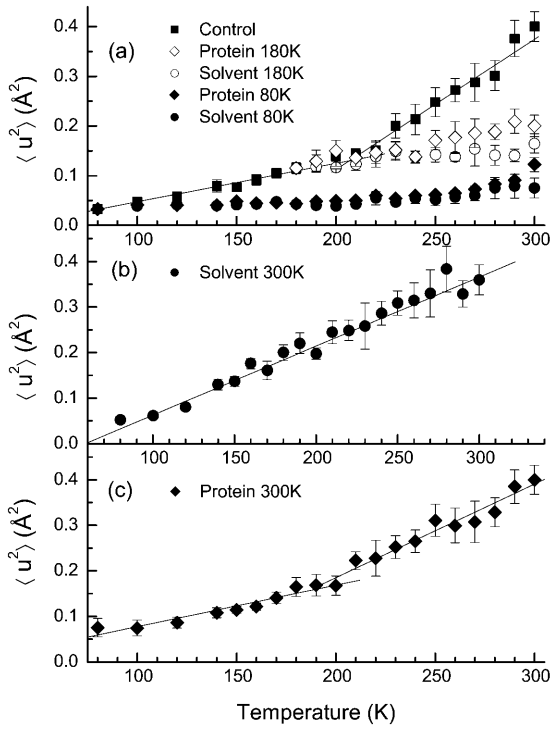

FIGURE 1 Mean-square fluctuations, $\langle u^2 \rangle$ of the protein nonhydrogen atoms for different sets of simulations. (*a*) ■, control set with protein and solvent at same temperature; ♦, protein held at 80 K; ●, solvent held at 80 K; ◇, protein held at 180 K; ○, solvent held at 180 K. (*b*) Solvent held at 300 K. (*c*) Protein held at 300 K. Standard errors were estimated by calculating the mean-square fluctuations for 10 bins each 20 ps long.

experimentally-known dynamical transition is reproduced, with nonlinearity starting at ~220 K. Fixing the solvent temperature at 80 K or 180 K suppresses the dynamical transition, the protein $\langle u^2 \rangle$ increasing linearly with temperature up to 300 K. Therefore, low temperature solvent cages the protein dynamics.

Fig. 1 *a* also shows that holding the protein temperature constant at 80 K or 180 K and varying the solvent temperature also abolishes the dynamical transition behavior in the protein. In summary, then, Fig. 1 *a* demonstrates that holding either component at a low temperature suppresses the protein dynamical transition.

Fig. 1, *b* and *c*, shows the effect of holding one component above the transition temperature while varying the temperature of the other. Holding the solvent temperature at 300 K (Fig. 1 *b*) leads to increased protein fluctuations at most temperatures relative to the other simulation sets. However, there is again no clear deviation from linearity, i.e., no dynamical transition behavior. In contrast, fixing the protein at 300 K and varying the solvent temperature (Fig. 1 *c*) recovers dynamical transition behavior in the protein, incipient at ~200 K, a slightly lower temperature than in the control set.

The above results are interpreted as follows. When fixing the solvent at 300 K, only effects due to changes with temperature in the sampled region of the protein energy

landscape appear. The absence of a dynamical transition indicates, then, that these changes do not control the transition. However, when the protein is held at 300 K, variations with temperature in the sampled solvent landscape trigger the protein transition.

The above finding of solvent control leads to the question of whether there is a radial dependence of the dynamical transition, i.e., to what extent solvent effects propagate into the protein center. To answer this, an analysis was performed of the dynamical transition behavior of classes of protein atoms in the control set of simulations. Initial calculations showed that side-chain atoms show stronger dynamical transition behavior than the backbone atoms (results not shown). Fig. 2 shows the side-chain fluctuations in the control simulations as a function of distance from the protein center of mass. The dynamical transition is seen to be most pronounced in the outer parts of the protein, i.e., those close to the solvent shell—above the transition the outer shells exhibit both stronger fluctuations and a larger change in gradient (inset, Fig. 2) than the inner atoms.

Finally, we ask the question of which properties of the solvent are responsible for inducing the protein transition. To examine this, the translational diffusion constant and dipole rotational correlation times were calculated for the water molecules (Figs. 3, 4, and 5).

Fig. 3 shows that there is a qualitative transition in the temperature dependence of the water translational diffusion constant at the dynamical transition. If the diffusion behaves as an activated process i.e., $D_{\text{trans}} \propto \exp(-a/T)$, then straight line behavior in the inset to Fig. 3 would be expected. What is seen is two regimes of linear behavior, below and above the transition, involving a lowering of the effective activation energy for water translational diffusion above the transition. This is true even when the protein atoms are fixed, showing that this water transition is inherent to the solvent shell and is

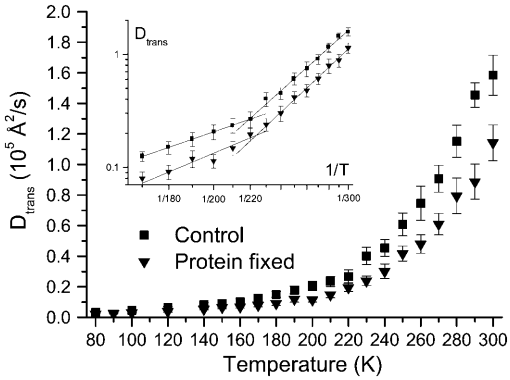

FIGURE 3 Translational diffusion constant, D_{trans}, for different sets of simulations. $D_{\text{trans}} = \lim_{\Delta t \to \infty} \langle |\mathbf{r}(\Delta t + t_0) - \mathbf{r}(t_0)|^2 / 6\Delta t \rangle_{t_0}$, where $\mathbf{r}(t)$ is the position of a water molecule oxygen atom at time interval Δt after an initial time t_0. For practical reasons Δt was set to 20 ps. D_{trans} was calculated as the mean over 10 time intervals each 20 ps long. The errors were estimated using the standard deviation over the 10 intervals. (■) Protein and solvent at same temperature; (▼) protein held fixed. *Inset*: the same data plotted as log D_{trans} versus $1/T$. Straight line fits below and above 220 K are also shown.

independent of the protein dynamics. The linear D_{trans} versus T scale on Fig. 3 makes clear that above the transition the translational diffusion increases rapidly with temperature.

Fig. 4 compares the excess water translational diffusion constant, i.e., that over and above the effective diffusion constant for harmonic motion (see caption to Fig. 4) with the excess mean-square fluctuation of the protein (again, the excess over the harmonic part). The two quantities vary nearly identically with temperature. Thus, water translational diffusion is seen to drive the protein dynamical transition.

Fig. 5 shows that when the protein is fixed, the water dipole rotational autocorrelation time undergoes no change through the dynamical transition. Thus the water rotational reorientation is completely decoupled from the transition in

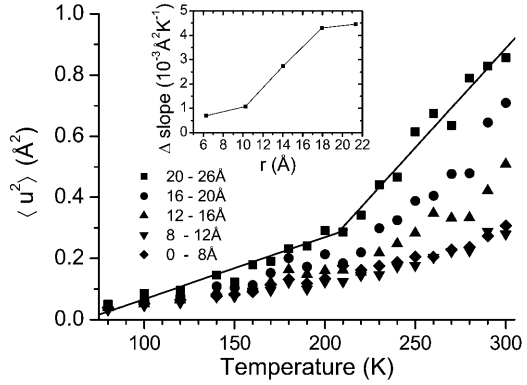

FIGURE 2 Mean-square fluctuations of the protein side-chain heavy atoms for five different shells, each 4 Å thick (except for the inner shell (8 Å) and outer shell (6 Å)). The inset shows the difference in slopes of lines fitted below and above 220 K as a function of distance from the protein center of mass. Linear fits to the data above and below 220 K are also shown for the outermost shell.

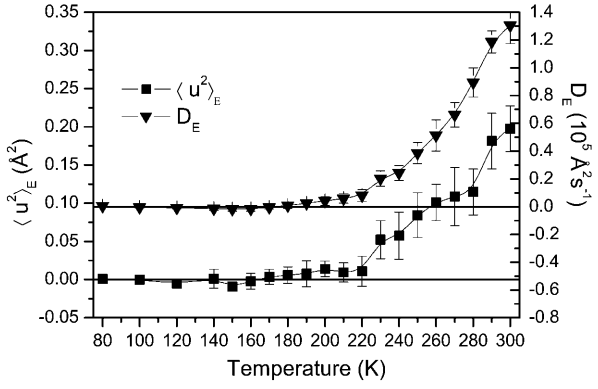

FIGURE 4 Excess mean-square fluctuation, $\langle u^2 \rangle_E$ and excess water translational diffusion constant, D_E versus temperature. $\langle u^2 \rangle_E$ is defined as $\langle u^2 \rangle - \langle u^2 \rangle_H$ where $\langle u^2 \rangle_H$ is the linear part of $\langle u^2 \rangle$ obtained by fitting to the data below 220 K. D_E is calculated from $D_{\text{trans}} - D_H$ where D_H is the linear part of D_{trans} obtained by fitting to the data below 220 K. All data calculated from the control simulations (protein and solvent at the same temperature).

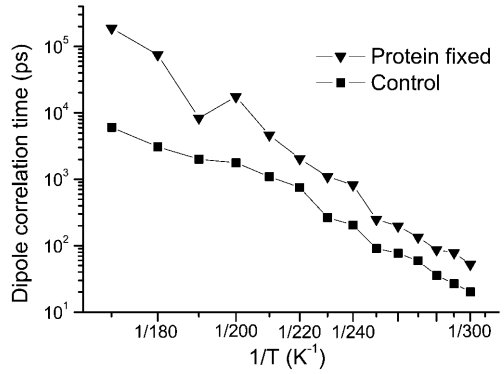

FIGURE 5 Dipole rotational autocorrelation time on a logarithmic scale versus $1/T$. The dipole rotational autocorrelation time was calculated by fitting to the correlation function $\langle\cos(\theta(t))\rangle$ where $\cos(\theta(t))$ denotes the scalar product of the corresponding dipole vectors of unit length separated by a time t. The correlation times were calculated by fitting the correlation curves between 1.5 and 20 ps with a stretched exponential function. (■) protein and solvent at same temperature (control); (▼) protein fixed.

the translational diffusion seen in this simulation. In the control simulations a small change in slope in Fig. 5 is seen, suggesting a change in the rotational properties. However, this change is much smaller and less sharp than that seen for translational diffusion.

CONCLUSION

It has been shown by MD simulation that a protein in vacuum undergoes a dynamical transition (Smith et al., 1990; Hayward and Smith, 2002). Deviation from linear behavior of $\langle u^2\rangle$ versus T occurs at very low temperatures (120 K) in isolated BPTI, although no clearly-demarcated dynamical transition at 220 K exists (Hayward and Smith, 2002).

In the case of a hydrated protein, equilibrium (potential of mean force) solvation effects can, in principle, modify the effective protein potential surface. A qualitative change in hydration water shell dynamics has been seen in MD simulation (Bizzarri et al., 2000). Decoupling of ''rattling'' motions from more global translational diffusion also was observed and is a characteristic of the glass transition (Angell, 1995), indicating that the water transition is also glasslike. The solvent transition is also found in this work. Moreover, it is found to be independent of the protein dynamics in that it is present even in simulations in which the protein atoms are fixed. The solvent transition involves activation of translational diffusion without a clear change in the water reorientational dynamics. MD work on ribonuclease showed that inhibiting the solvent translational mobility, and therefore the protein-water hydrogen-bond dynamics, reduces protein atomic fluctuations at 300 K (Tarek and Tobias, 2002).

The above observations raise the question of whether the solvent translational diffusion is responsible for the change in slope of $\langle u^2\rangle$ versus T in the protein, i.e., the protein dynamical transition itself. The present results provide an affirmative answer to this question. It is shown here that the dynamical transition of a protein when hydrated is driven by changes with temperature in the solvent dynamics. This is proven by the finding that holding the solvent at high or low temperatures abolishes the protein dynamical transition, whereas varying the solvent temperature with the protein held at 300 K recovers it.

This work builds upon intriguing dual heatbath MD simulations on the same system by Vitkup et al. (2000). The results presented here agree with the findings in Vitkup et al. (2000) that solvent held at low temperature inhibits protein dynamics. However, in Vitkup et al. (2000) a key conclusion is that when the protein is held at 180 K but the solvent at 300 K then the protein fluctuations are almost identical to those at 300 K. In contrast to this, the protein 180 K simulations in Fig. 1 *a* clearly show that the protein fluctuations when the solvent is at 300 K are only ~50% of those in the control set at 300 K. Fig. 1 *a* also shows that holding the protein temperature at 180 K while varying the solvent temperature abolishes the dynamical transition in the protein.

In the series of hot solvent (300 K) simulations in this work (Fig. 1 *b*) the solvent does increase the protein fluctuations, by ~20–50% relative to the control, for temperatures below ~250 K. The solvent may soften the effective potential seen by the protein atoms (or, in the language of Zaccai (2000), it reduces the ''resilience'' of the protein). One sees, at the same time, that keeping the solvent hot abolishes the 220 K dynamical transition in the protein. The present results suggest that this is due to the fact that, in the hot solvent simulations, translational solvent diffusion is not specifically enhanced above 220 K.

The solvent transition drives dynamical transition behavior primarily in the side-chain atoms of the external protein regions, i.e., those closest to the solvent. This dovetails with the recently proposed ''radially-softening'' description of protein dynamics, based on MD-simulation analysis of quasielastic neutron scattering data, in which it was shown that the average dynamical properties of a protein at 300 K vary smoothly with increasing distance from the protein core, involving a gradual increase of the diffusive amplitudes and a narrowing and shift to shorter (ps) times of the distribution of diffusive relaxation processes (Dellerue et al., 2001).

REFERENCES

Angell, C. A. 1995. Formation of glasses from liquids and biopolymers. *Science*. 267:1924–1935.

Bicout, D. J., and G. Zaccai. 2001. Protein flexibility from the dynamical transition: a force constant analysis. *Biophys. J.* 80:1115–1123.

Bizzarri, A. R., A. Paciaroni, and S. Cannistraro. 2000. Glasslike dynamical behavior of the plastocyanin hydration water. *Phys. Rev. E.* 62:3991–3999.

Brooks, B. R., R. E. Bruccoleri, B. D. Olafson, D. J. States, S. Swaminathan, and M. Karplus. 1983. CHARMM: a program for

macromolecular energy, minimization and dynamics calculations. *J. Comput. Biol.* 4:187–217.

Caliskan, G., A. Kisliuk, and A. P. Sokolov. 2002. Dynamic transition in lysozyme: role of a solvent. *Journal of Non-Crystalline Solids.* 307–310:868–873.

Cohen, S. G., E. R. Bauminger, I. Nowik, S. Ofer, and J. Yariv. 1981. Dynamics of the iron-containing core in crystals of the iron-storage protein, ferritin, through Mossbauer spectroscopy. *Phys. Rev. Lett.* 46:1244–1248.

Cordone, L., M. Ferrand, E. Vitrano, and G. Zaccai. 1999. Harmonic behavior of trehalose-coated carbon-monoxy-myoglobin at high temperature. *Biophys. J.* 76:1043–1047.

Dellerue, S., A. J. Petrescu, J. C. Smith, and M. C. Bellissent-Funel. 2001. Radially softening diffusive motions in a globular protein. *Biophys. J.* 81:1666–1676.

Doster, W., S. Cusack, and W. Petry. 1989. Dynamical transition of myoglobin revealed by inelastic neutron scattering. *Nature.* 337:754–756.

Doster, W., S. Cusack, and W. Petry. 1990. Dynamic instability of liquidlike motions in a globular protein observed by inelastic neutron scattering. *Phys. Rev. Lett.* 65:1080–1083.

Ferrand, M., A. J. Dianoux, W. Petry, and G. Zaccai. 1993. Thermal motions and function of bacteriorhodopsin in purple membranes: effects of temperature and hydration studied by neutron scattering. *Proc. Natl. Acad. Sci. USA.* 90:9668–9672.

Fitter, J. 1999. The temperature dependence of internal molecular motions in hydrated and dry alpha-amylase: the role of hydration water in the dynamical transition of proteins. *Biophys. J.* 76:1034–1042.

Fitter, J., R. E. Lechner, and N. A. Dencher. 1997. Picosecond molecular motions in bacteriorhodopsin from neutron scattering. *Biophys. J.* 73: 2126–2137.

Green, J. L., J. Fan, and C. A. Angell. 1994. The protein-glass analogy: some insights from homopeptide comparisons. *J. Phys. Chem.* 98: 13780–13790.

Hagen, S. J., J. Hofrichter, and W. A. Eaton. 1995. Protein reaction kinetics in a room-temperature glass. *Science.* 269:959–962.

Hayward, J. A., and J. C. Smith. 2002. Temperature dependence of protein dynamics: computer simulation analysis of neutron scattering properties. *Biophys. J.* 82:1216–1225.

Holian, B. L., A. F. Voter, and R. Ravelo. 1995. Thermostatted molecular dynamics: how to avoid the Toda demon hidden in Nose-Hoover dynamics. *Phys. Rev. E.* 52:2338–2347.

Hoover, W. G. 1985. Canonical dynamics: Equilibrium phase-space distributions. *Phys. Rev. A.* 31:1695–1697.

Jorgensen, W. L., J. Chandrasekhar, J. D. Madura, R. W. Impey, and M. L. Klein. 1983. Comparison of simple potential functions for simulating liquid water. *J. Chem. Phys.* 79:926–934.

Knapp, E. W., S. F. Fischer, and F. Parak. 1982. Protein dynamics from Mossbauer spectra. The temperature dependence. *J. Am. Chem. Soc.* 86:5042–5047.

Lee, A. L., and A. J. Wand. 2001. Microscopic origins of entropy, heat capacity and the glass transition in proteins. *Nature.* 411:501–504.

MacKerell, A. D., Jr., D. Bashford, M. Bellott, R. L. Dunbrack, Jr., J. D. Evanseck, M. J. Field, S. Fischer, J. Gao, H. Guo, S. Ha, D. Joseph-McCarthy, L. Kuchnir, K. Kuczera, F. T. K. Lau, C. Mattos, S. Michnick, T. Ngo, D. T. Nguyen, B. Prodhom, W. E. Reiher III, B. Roux, M. Schlenkrich, J. C. Smith, R. Stote, J. Straub, M. Watanabe, J. Wiórkiewicz-Kuczera, D. Yin, and M. Karplus. 1998. All-atom empirical potential for molecular modelling and dyamics studies of proteins. *J. Phys. Chem.* 102:3586–3616.

Martyna, G. J., M. E. Tuckerman, D. J. Tobias, and M. L. Klein. 1996. Explicit reversible integrators for extended systems dynamics. *Molecular Physics.* 87:1117–1157.

Paciaroni, A., S. Cinelli, and G. Onori. 2002. Effect of the environment on the protein dynamical transition: a neutron scattering study. *Biophys. J.* 83:1157–1164.

Parak, F., E. N. Frolov, A. A. Kononenko, R. L. Mossbauer, V. I. Goldanskii, and A. B. Rubin. 1980. Evidence for a correlation between the photoinduced electron transfer and dynamic properties of the chromatophore membranes from Rhodospirillum rubrum. *FEBS Lett.* 117:368–372.

Parak, F., E. N. Frolov, R. L. Mossbauer, and V. I. Goldanskii. 1981. Dynamics of metmyoglobin crystals investigated by nuclear gamma resonance absorption. *J. Mol. Biol.* 145:825–833.

Rasmussen, B. F., A. M. Stock, D. Ringe, and G. A. Petsko. 1992. Crystalline ribonuclease A loses function below the dynamical transition at 220 K. *Nature.* 357:423–424.

Reat, V., R. Dunn, M. Ferrand, J. L. Finney, R. M. Daniel, and J. C. Smith. 2000. Solvent dependence of dynamic transitions in protein solutions. *Proc. Natl. Acad. Sci. USA.* 97:9961–9966.

Smith, J., K. Kuczera, and M. Karplus. 1990. Dynamics of myoglobin: comparison of simulation results with neutron scattering spectra. *Proc. Natl. Acad. Sci. USA.* 87:1601–1605.

Steinbach, P. J., and B. R. Brooks. 1993. Protein hydration elucidated by molecular dynamics simulation. *Proc. Natl. Acad. Sci. USA.* 90:9135–9139.

Steinbach, P. J., and B. R. Brooks. 1996. Hydrated myoglobin's anharmonic fluctuations are not primarily due to dihedral transitions. *Proc. Natl. Acad. Sci. USA.* 93:55–59.

Tarek, M., and D. J. Tobias. 2000. The dynamics of protein hydration water: a quantitative comparison of molecular dynamics simulations and neutron-scattering experiments. *Biophys. J.* 79:3244–3257.

Tarek, M., and D. J. Tobias. 2002. Role of protein-water hydrogen bond dynamics in the protein dynamical transition. *Phys. Rev. Lett.* 88:138101.

Teeter, M. M., A. Yamano, B. Stec, and U. Mohanty. 2001. On the nature of a glassy state of matter in a hydrated protein: Relation to protein function. *Proc. Natl. Acad. Sci. USA.* 98:11242–11247.

Tilton, R. F., Jr., J. C. Dewan, and G. A. Petsko. 1992. Effects of temperature on protein structure and dynamics: X-ray crystallographic studies of the protein ribonuclease-A at nine different temperatures from 98 to 320 K. *Biochemistry.* 31:2469–2481.

Vitkup, D., D. Ringe, G. A. Petsko, and M. Karplus. 2000. Solvent mobility and the protein glass' transition. *Nat. Struct. Biol.* 7:34–38.

Vojtechovsky, J., K. Chu, J. Berendzen, R. M. Sweet, and I. Schlichting. 1999. Crystal structures of myoglobin-ligand complexes at near-atomic resolution. *Biophys. J.* 77:2153–2174.

Walser, R., A. E. Mark, and W. F. van Gunsteren. 2000. On the temperature and pressure dependence of a range of properties of a type of water model commonly used in high-temperature protein unfolding simulations. *Biophys. J.* 78:2752–2760.

Zaccai, G. 2000. How soft is a protein? *Science.* 288:1604–1607.